Hindawi
Advances in Materials Science and Engineering
Volume 2019, Article ID 8053843, 19 pages
https://doi.org/10.1155/2019/8053843

Review Article

Microstructure Characteristics of GFRP Reinforcing Bars in Harsh Environment

Hilal El-Hassan and Tamer El Maaddawy

Department of Civil and Environmental Engineering, UAE University, Al Ain, Abu Dhabi, P.O. Box 15551, UAE

Correspondence should be addressed to Hilal El-Hassan; helhassan@uaeu.ac.ae

Received 15 January 2019; Revised 5 March 2019; Accepted 13 March 2019; Published 1 April 2019

Guest Editor: Alena Šišková

Fiber reinforced polymer (FRP) composites have been suggested as corrosion-resistant alternatives to traditional steel reinforcement in concrete structures. Within this family of composites, glass fiber reinforced polymers (GFRPs) have been gaining momentum as the primary selection of FRP for construction applications. Despite being advantageous, its wide adoption by the industry has been hindered due to the degradation of its performance in severe environmental conditions. As such, significant studies have been carried out to assess the mechanical properties of GFRP bars subject to different conditioning schemes. However, the inconsistencies and wide variations of results called for more in-depth microstructure evaluation. Accordingly, this paper presents a critical review of existing research on the microstructure of GFRP reinforcing bars exposed to various conditioning regimes. The review analysis revealed that sustained load limits set by codes and standards were satisfactory for nonaggressive environment conditions but should be updated to include different conditioning regimes. It was also found that conditioning in alkaline solutions was more severe than concrete and mortars, where test specimens experienced irreversible chemical degradation, more hydroxyl group formation, and more intense degradation to the microstructure. The progression of hydrolysis was reported correlatively through an increase in hydroxyl groups and a decrease in the glass transition temperature. While moisture uptake was the primary instigator of hydrolysis, restricting it to 1.6% could limit the reduction in tensile strength to 15%. Further, the paper identifies research gaps in the existing knowledge and highlights directions for future research.

1. Introduction

Reinforced concrete structures are designed with certain life expectancy under normal service conditions. However, exposure to severe environments may reduce the design service life due to unanticipated durability problems, including corrosion of steel reinforcement. The corrosion of steel reinforcing bars causes cracking and spalling of concrete, creating major reductions in performance and a significant increase in cost for rehabilitation. In fact, Koch [1] reported that 3-4% of each nation's gross domestic product is dedicated to corrosion-related expenditures. As a form of corrosion management, glass fiber reinforced polymer (GFRP) reinforcing bars have been proposed as a replacement to steel equivalents. This alternative reinforcement is characterized by its light weight, high strength-to-weight ratio, and corrosion resistance [2–4]. However, conflicting results on the degradation of its properties upon exposure to alkaline or acidic solution, moisture/water, and elevated temperatures have been a major setback in its adoption by the construction industry [2–4].

For the last few years, extensive research has been carried out to investigate the durability performance of GFRP reinforcement exposed to different environmental conditions. Research findings have identified the major contributors to deterioration of GFRP as moisture uptake, alkaline environment, and temperature. Moisture penetrates the matrix by the flow of solution into the microgaps between polymer chains and capillary transport through fiber/matrix interfacial microcracks and in microcracks formed during manufacturing [5]. As a result, the matrix exhibits plasticisation, leading to a reduction in strength and glass

transition temperature. On the other hand, alkaline solutions break the bond between the oxygen and carbon atoms in the molecular chain of the GFRP matrix. This breakage creates microcracks and fractures in the matrix structure, leading to more moisture uptake and a significant reduction in strength. Further, to expedite investigative work conducted on GFRP reinforcing bars, higher temperatures have been employed. Vijay and GangaRao [6] reported that an increase in the conditioning temperature led to an exponential amplification in the actual age. Nevertheless, it should be noted that the elevated temperatures employed in most work may have affected the physical properties of the bars by increasing the coefficient of thermal expansion [7] and, thus, may have altered the behavior of the GFRP bars, rendering the results, in some cases, unrealistic.

With the majority of past work characterizing the durability performance of GFRP bars, several researchers have reviewed and summarized these publications to highlight the gaps in existing knowledge and propose future direction of research. In contrast, much fewer and more recent investigations have correlated the degradation in GFRP to changes in the microstructure. Yet, there is no such review and summary of these in-depth investigations. Accordingly, this paper aims to present an overview of recent studies examining the effect of conditioning on the microstructure of GFRP reinforcing bars. Research findings obtained help to shed light on the morphological and microstructure changes in GFRP bars subject to different exposure conditions using various microstructure characterization techniques, including differential scanning calorimetry (DSC), thermogravimetric analysis (TGA), Fourier transform infrared spectroscopy (FTIR), and scanning electron microscopy (SEM). A correlation among these microstructural evaluation techniques is reported. The influence of moisture uptake on the microstructure of conditioned GFRP bars is also evaluated.

2. Taxonomy

GFRP reinforcing bars are made of glass fibers impregnated with an organic resin or matrix. Typical diameters range between 8 and 20 mm with smooth surfaces for smaller sizes and ribbed and/or sand-coated surfaces for larger counterparts. GFRP reinforcement falls within the family of FRP composites. The taxonomy on the studies of FRP composites is presented in Figure 1. They can be classified based on their fiber type, resin type, and application. Different combinations of fibers and resins have been employed in the production of FRPs, of which composites made with glass fibers and vinylester are the most common. Also, FRPs have been used across many industries, including aerospace, automotive, sports, musical, and construction. In the latter industry, they have been employed in new and existing buildings as internal and external reinforcing bars and for repair, strengthening, and retrofitting purposes. The literature has especially focused on the ability of FRPs to replace steel as the main reinforcement in concrete structures [8–15]. However, before being widely adopted by the construction industry, their durability performance was rigorously investigated. Accordingly, GFRP reinforcing bars have been conditioned in various media, including acidic and alkaline solutions, concrete, tap water, and seawater. Elevated temperatures were also employed during conditioning to accelerate the degradation process. Further, the validity of the environmental reduction factors and creep rupture stress limits adopted by the current international guidelines and standards were assessed by applying a sustained load to GFRP bars exposed to severe environments. Such specimens were examined for performance retention by measuring the tensile properties after conditioning. Correlations between the properties and microstructural changes were evaluated using DSC, TGA, SEM, FTIR, and moisture uptake.

3. GFRP Reinforcing Bars

The properties of GFRP reinforcing bars and conditions to which they are exposed are primary factors affecting their performance and microstructure. As such, a comprehensive review of the literature on the physical and mechanical properties and conditioning of GFRP bars is presented in the sections below. It should be noted that the literature reviewed in this paper focuses on examining the microstructure characteristics of GFRP bars exposed to different conditioning regimes.

3.1. Physical Properties. Prior to conducting any experimental testing on GFRP reinforcing bars, their physical properties were determined. Various tests, shown in Table 1, were typically carried out to measure the diameter, void content, fiber content, moisture uptake, glass transition temperature, and thermal expansion coefficient. Physical properties reported in past studies are summarized in Table 2. The most commonly used glass and matrix materials were E-glass and vinylester, with 90 and 74% of the conducted research having used this fiber and matrix, respectively, as shown in Figure 2. Epoxy, on the other hand, has been only recently employed as the resin of GFRP reinforcing bars, with 14% of published work having explored its combination with E-glass [8, 10, 11, 23, 41, 42]. The diameter has also been varied between 8 and 44.5 mm, with the majority being approximately 12 mm. Yet, Benmokrane, et al. [24] concluded that the bar diameter had limited influence on the physical and mechanical properties of GFRP reinforcing bars. Furthermore, very limited work reported the thermal expansion coefficients, as it was not typically measured by researchers, but provided by the manufacturer [8, 13, 14, 24–27]. In contrast, the moisture uptake has been essential in characterizing the performance and assessing its retention capacity. It ranged between 0.01 and 1.59%, by mass, for unconditioned/control specimens. The fiber content was measured by volume and mass. However, the latter was more commonly reported with the availability of standardized test procedures (ASTM D3171 and ASTM E1868). Measured values ranged between 70 and 83%. The volumetric fiber content, on the other hand, was mainly provided by the manufacturer and could only be determined at the initial stages of production.

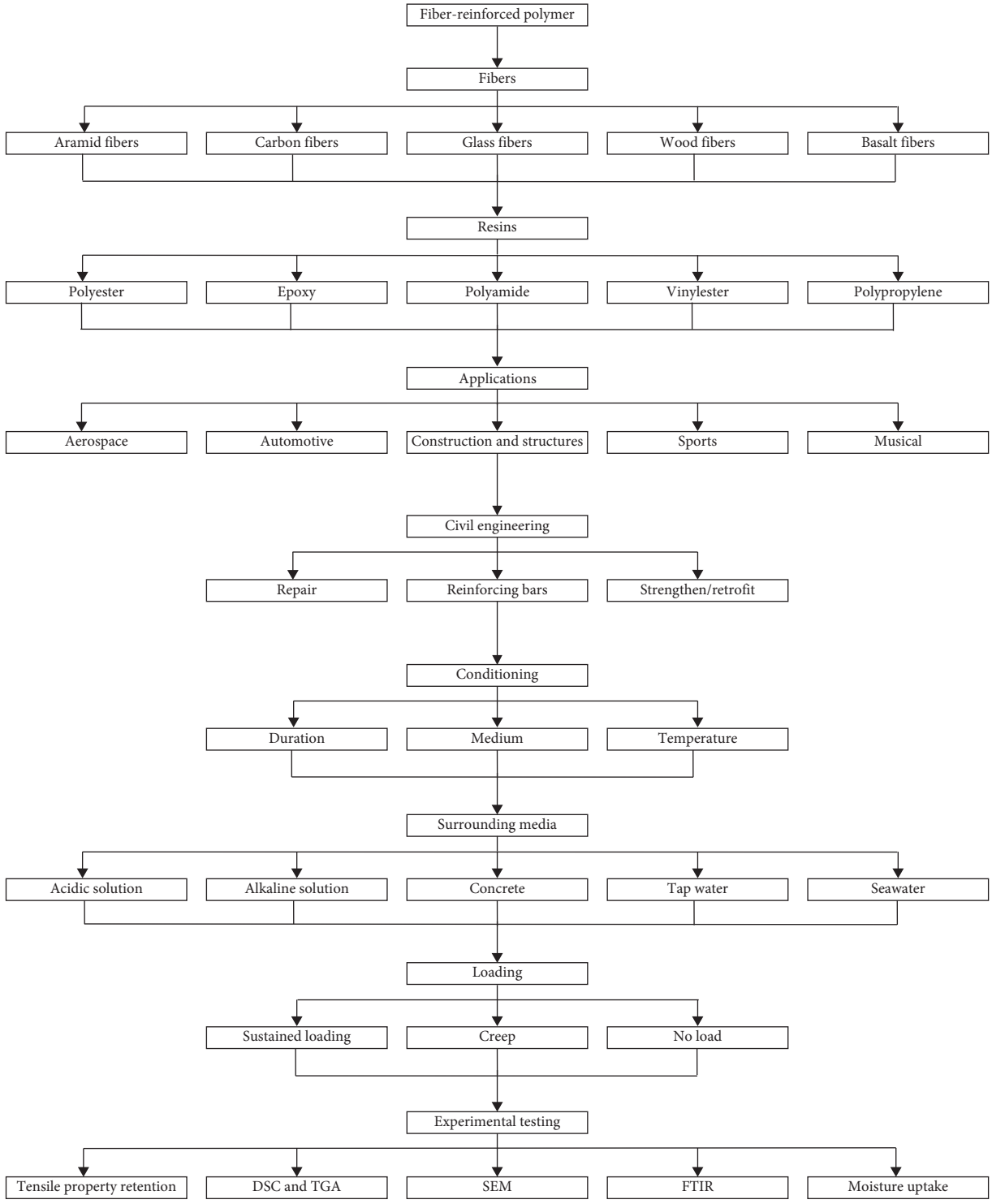

Figure 1: Taxonomy on the studies of fiber reinforced polymer composites.

3.2. Mechanical Properties. The performance of GFRP reinforcing bars is typically characterized by its ability to retain its mechanical properties. For this reason, as-received and unconditioned specimens were tested for various performance indicators, as summarized in Table 3, including tensile and flexural strength, strain, and modulus. Shear strength was also reported in relevant work. Experimental results of a number of studies are shown in Table 4. Over 90% of the studies focused on tensile properties, with values of tensile strength, modulus, and strain in the range of 432–1321 MPa, 31–65 GPa, and 1–3%, respectively. Given the large database of results for the former two properties, it was possible to develop a relation between them. Figure 3 presents a correlation between tensile modulus (E_t) and

Table 1: Summary of standardized testing for physical properties.

Property (unit)	Standardized test	Reference
Diameter (mm)	ACI 440.3R & ASTM D7205	[3, 16]
Void content (%)	ASTM D3171 & ASTM D2734	[17, 18]
Fiber content, by mass (%)	ASTM D3171 & ASTM E1868	[17, 19]
Moisture uptake (%)	ASTM D570	[20]
Glass transition temperature (°C)	ASTM E1356	[21]
Thermal expansion coefficient (/°C)	ASTM E831	[22]

Table 2: Physical properties of GFRP reinforcing bars.

Reference	Glass material	Matrix material	Diameter (mm)	Long. thermal expansion coef. (x 10^{-6}/°C)	Trans. thermal expansion coef. (x 10^{-6}/°C)	Moisture absorption (%)	Fiber content (%, by volume)	Fiber content (%, by mass)
[7]	E-glass	Vinylester	9.5	—	—	0.1	—	74.5
[8]	E-glass	Vinylester polyester epoxy	12	—	17.7–20.8	0.23–1.15	—	78.8–83.9
[9]	Short Glass E-glass	Vinylester	15.0–20.0	—	—	—	—	83
[10]	E-glass	Epoxy	8.0–9.0	—	—	0.1	—	75.5–78.3
[11]	E-glass	Epoxy	8.0–9.0	—	—	0.10	—	75–78
[12]	E-glass E-glass 366 Advantex 366 Advantex 712	Polyester vinylester	9.3–12.0	—	—	0.01–0.05	—	—
[13]	E-glass	Vinylester	19.0	6.1	23.5	0.48	65.4	74.5
[14]	E-glass	Vinylester	12.7	5.5	29.5	0.38	60.3	77.9
[15]	E-glass	Vinylester	9.5	—	—	—	65	—
[23]	E-glass	Vinylester polyester epoxy	12	—	—	0.23–1.15	—	78.8–83.9
[24]	E-glass	Vinylester	9.5–25.4	—	20.5–22.0	0.02–0.15	80.9–83.0	—
[25]	E-glass	Vinylester	12.7	6.7	27.2	0.62	64.3	81.5
[26]	E-glass	Vinylester	12.7	5.5	29.5	0.38	—	77.9
[27]	E-glass	Vinylester polyester	25.4–44.5	6.9–7.8	21.0–27.1	0.05–1.59	—	79.6–81.5
[28]	E-glass	Vinylester	8.0	—	—	—	—	—
[29]	E-glass	Vinylester	9	—	—	—	70	—
[30]	E-glass	Vinylester	12	—	—	—	—	83
[31]	E-glass	Epoxy	14	—	—	0.01	—	—
[32]	E-glass	Vinylester	12	—	—	—	—	83
[33]	E-glass	Vinylester	9.5	—	—	—	—	—
[34]	E-glass	Vinylester	12.7	—	—	0.37	—	81.5
[35]	E-glass	Vinylester	9.5–16.0	—	—	—	75	—
[36]	E-glass	Vinylester	12.7	—	—	—	—	69.1–73.3
[37]	E-glass	Vinylester	12	—	—	—	—	83
[38]	E-glass	Vinylester	—	—	—	—	—	—
[39]	E-glass	Vinylester	10	—	—	0.4	—	—
[40]	E-glass	Vinylester	—	—	—	—	—	—

square root of tensile strength ($\sqrt{f_t}$) of GFRP bars. A linear trend line, in the form of Equation (1) could provide a prediction of tensile modulus from the strength with reasonable accuracy. On the other hand, flexural and shear properties were recorded on few occasions, mainly in research work related to bending and shear testing. Yet, the available data have shown a linear relationship between flexural (f_r) and tensile strength (f_t), as shown in Figure 4 and Equation (2). This linear relation provides a reasonably accurate prediction of the former from the latter without the need for experimental testing. It is also worth noting that tensile properties of unconditioned GFRP samples made with epoxy as the matrix material seem to be, on average, 14% higher than those of vinylester counterparts. Additionally, a correlation was made between the physical and mechanical properties of GFRP specimens made with E-glass and vinylester. From Figure 5, it is clear that the tensile strength and modulus are generally proportional to the fiber content, up to a maximum value of 83%, by mass. Similarly, Micelli and Nanni [44] reported that GFRP bars

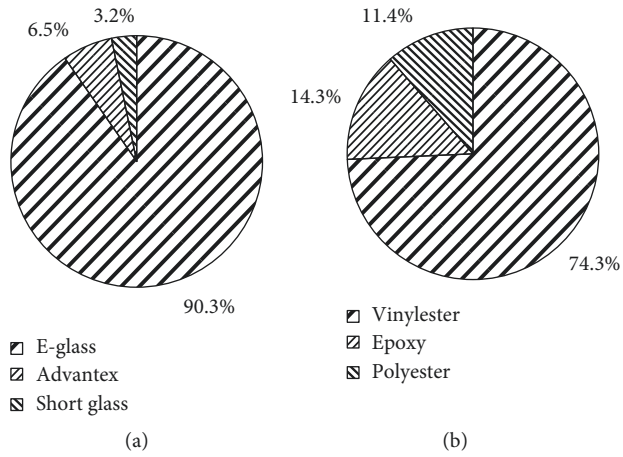

Figure 2: Percentage distribution of GFRP components. (a) Glass fiber material. (b) Matrix material.

Table 3: Summary of standardized testing for mechanical properties.

Mechanical property (unit)	Standardized test	Reference
Tensile strength (MPa)	ACI 440.3R & ASTM D7205	[3, 16]
Tensile strain (%)	ACI 440.3R & ASTM D7205	[3, 16]
Tensile modulus (MPa)	ACI 440.3R & ASTM D7205	[3, 16]
Flexural strength (MPa)	ASTM D4476	[43]
Flexural strain (%)	ASTM D4476	[43]
Flexural modulus (MPa)	ASTM D4476	[43]
Shear strength (MPa)	ACI 440.3R	[3]

with lower fiber content may experience inferior mechanical performance.

$$E_t = 1.67\sqrt{f_t}, \quad (1)$$

$$f_r = 1.28 f_t. \quad (2)$$

3.3. Conditioning. The durability performance of GFRP reinforcing bars exposed to different environmental conditions has been evaluated using accelerated aging tests. Four main exposure parameters were investigated: surrounding medium, conditioning duration, conditioning temperature, and presence of a sustained load. Table 5 summarizes the exposure conditions employed by various studies on the microstructure of GFRP bars. It should be noted that only one study reviewed in this work, assessing the microstructure, has investigated the effect of acidic solutions on the performance of GFRP. Seawater exposure has also received little attention, although it is critical to assess the properties and microstructure of GFRP bars for employment in offshore structures and bridge decks in coastal cities and seaports [10, 11, 42]. According to Figure 6(a), alkaline and water solutions have been utilized in 39 and 25% of the studies shown herein. It seems that the ease of preparing such media renders them most favourable among researchers, especially that the former is proposed to simulate concrete alkalinity and behavior. Concrete, on the other hand, has been used by 23% of presented research, even though it better represents real-life scenarios.

The duration of conditioning has been widely altered in research studies and ranged between 0.02 and 7200 days. Figure 6(b) shows that 28, 18, 10, 23, and 21% of studies have conditioned GFRP bars for a maximum of 0–90, 91 to 180, 181 to 240, 241 to 365, and more than 365 days, respectively. Clearly, the majority of research has focused on examining the effects of early age and prolonged conditioning.

The conditioning temperature has been pivotal in accelerating aging of GFRP specimens. Work by Vijay and GangaRao [6] highlighted the relationship between actual age in calendar days at Morgantown, WV, and chamber conditioning days in the form of Equation (3), where T is the temperature in °F. It is worth noting that in their experiments, they [6] placed the specimens in a weathering chamber, i.e., a controlled temperature environment, and in alkaline solutions. Effectively, an increase in chamber conditioning temperature (T) led to an amplification in the actual age. Thus, the conditioning temperature has been altered within and among different studies. In general, they have ranged between 20°C and 90°C, with the exceptions of [25, 32], which investigated the performance of GFRP bars subject to freezing and elevated temperatures. Based on Equation (3), such conditioning temperatures (20°C–90°C) could accelerate the aging by at least four times when specimens are conditioned in alkaline solutions. For instance, alkaline conditioning for 30 days in a chamber at 50°C is equivalent to an actual age of 2660 days (approx. 7 years) at Morgantown, WV. Yet, this equation may not be applicable to specimens encased in concrete or conditioned in regimes other than alkaline solutions. Figure 6(c) highlights the distribution of conditioning temperatures, with 77% of studies utilizing conditioning temperatures above 50°C. Nevertheless, it should be noted that such temperatures may affect the physical properties of the bars by increasing the coefficient of thermal expansion [7] and, thus,

Table 4: Mechanical properties of unconditioned GFRP reinforcing bars.

Reference	Tensile strength (MPa)	Tensile modulus (GPa)	Tensile strain (%)	Flexural strength (MPa)	Flexural modulus (GPa)	Flexural strain (%)	Shear strength (MPa)
[7]	653	38.5	—	888	—	—	—
[8]	—	—	—	1150–1573	56.9–663.3	2.02–2.54	250–270
[9]	1105–1184	62.6–64.7	1.71–1.89	—	—	—	—
[10]	816–1321	52–53	—	—	—	—	—
[11]	816–1321	52–53	—	—	—	—	—
[12]	612–958.3	31.6–51.8	—	—	—	—	—
[13]	728	47.6	1.53	—	—	—	—
[14]	786	46.3	1.7	1005	46.8	2.15	212
[15]	644.7	53.4	1.2	—	—	—	—
[23]	1015–1220	—	—	—	—	—	—
[24]	1237.4–1315.3	60.0–62.5	2.1–2.3	1406.3–1757.5	—	—	—
[25]	788	47.2	1.7	1095	52.6	2.15	185
[26]	786	46.3	1.7	—	—	—	—
[27]	—	—	—	759–1324	49.3–54.1	—	151–197
[28]	821	44.4	1.84	—	—	—	—
[29]	1200	42.9	2.8	—	—	—	—
[30]	1478	60.4	2.45	—	—	—	—
[31]	714.6	55	1.62	—	—	—	—
[32]	1478	60.4	2.45	—	—	—	—
[33]	700	40.8	—	—	—	—	—
[34]	854	43.0	—	—	—	—	—
[35]	580–658	40–42	1.4–1.6	—	—	—	—
[36]	660.6–692.8	38.5–42.7	—	—	—	—	36.9–42.3
[37]	432–1478	41.9–60.4	1.04–2.45	—	—	—	—

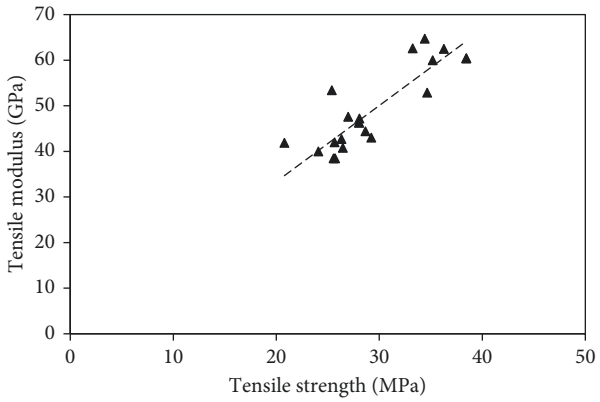

Figure 3: Relationship between tensile modulus and strength of GFRP bars.

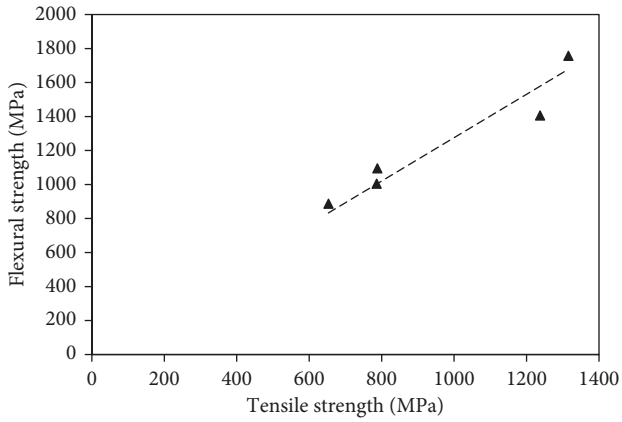

Figure 4: Correlation between flexural and tensile strength of GFRP bars.

may alter the behavior of the GFRP bars, rendering unrealistic results.

$$\frac{\text{Age in calendar days}}{\text{Chamber conditioning days}} = 0.098e^{0.0558T}. \quad (3)$$

3.4. Loading. The degradation of GFRP reinforcing bars could be intensified in the presence of a sustained load during conditioning [53–55]. ACI 440.1R [2] limits the tensile stress in GFRP under service conditions to 14% of the ultimate tensile strength (UTS), considering the strength reduction factor for environmental exposure. Higher stress levels caused a shift in the degradation mechanism of GFRP from being affected by the rate of diffusion of alkaline solutions to being controlled by solution transport through resin cracks [56]. Nevertheless, it can be noted from Figure 6(d) that only 27% of investigated microstructure studies applied a sustained load to GFRP bars, with values ranging from 0 to 80% UTS. The objectives of these works, nonetheless, were different. While some researchers applied sustained loads within the limits specified by codes and standards [2, 4, 57–60], others explored the possibility of increasing this allowable limit [11, 12, 28, 33–35, 52]. Some of these latter studies concluded that the limits recommended by codes and standards were conservative for specific reinforcing bars and conditions. In fact, elevated temperatures could accelerate the degradation induced by conditioning. As a result, the limits were found to be

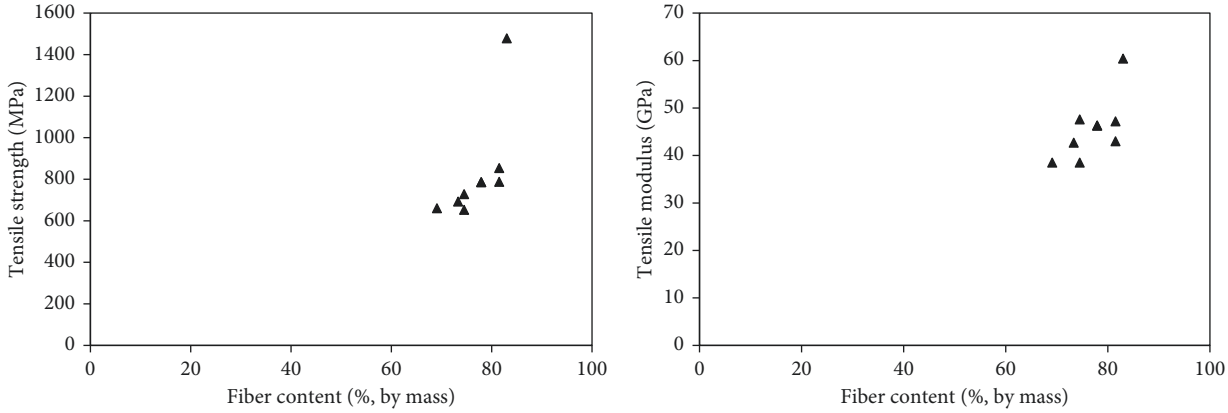

Figure 5: Correlation between fiber content and mechanical properties. (a) Tensile strength. (b) Tensile modulus.

Table 5: Summary of conditioning regimes in studies investigating the microstructure of GFRP reinforcing bars.

Reference	Surrounding media					Conditioning		Loading	
	Alkaline	Concrete	Water	Seawater	Acidic	Duration (days)	Temperature (°C)	Yes (%, UTS[1])	No
[7]			x			40 to 120	23 to 80		x
[8]	x					41.7 to 208.3	60		x
[9]	x	x				30 to 60	−30 to 60		x
[10]		x		x		150 to 450	20 to 60		x
[11]		x		x		150 to 450	20 to 60	25	
[12]	x	X				Up to 1445	–	20–65	
[13]			x			60 to 180	23 to 50		x
[14]		x	x			60 to 240	23 to 50		x
[15]	x					100 to 660	40		x
[23]	x					41.67 to 208.33	22 to 60		x
[42]				x		90 to 365	23 to 65		x
[24]	x					90	60		x
[25]			x			0.0208 to 0.1285	−100 to 325		x
[26]	x	x				60 to 365	23 to 70		x
[27]	x					30 to 180	23 to 60		x
[28]	x					30 to 270	23	0–25	
[29]	x		x	x	x	28 to 50	60 to 80		x
[30]	x		x	x		180 to 540	23 to 50		x
[31]	x					30 to 720	60		x
[32]		x				0.0417 to 0.125	100 to 300		x
[33]	x	x	x			90 to 730	60	20 & x[2]	
[34]		x	x			60 to 240	23 to 50	20–80	
[35]	x		x			30 to 120	20 to 73	19–29	
[36]	x		x	x		30 to 132	−25 to 80		x
[37]		x	x	x		180 to 540	23 to 50		x
[38]		x[2]				1825 to 2920	−24 to 30	x[2]	
[39]	x					30 to 365	23 to 75		x
[40]	x		x			54.2	22 to 90		x
[44]	x	x				21 to 42	−18 to 49		x
[45]	x		x			15 to 60	60		x
[46]	x		x			42 to 365	20 to 60	15	
[47]		x				30 to 270	20 to 60	10–15	
[48]	x					30 to 180	60		x
[49]	x					41.7	60		x
[50]	x					20 to 120	20 to 70		x
[51]			x	x		41.7	20 to 70		x
[52]	x	x	x			90 to 730	60	20 & x[1]	

[1]Ultimate tensile strength. [2]Natural weathering conditions.

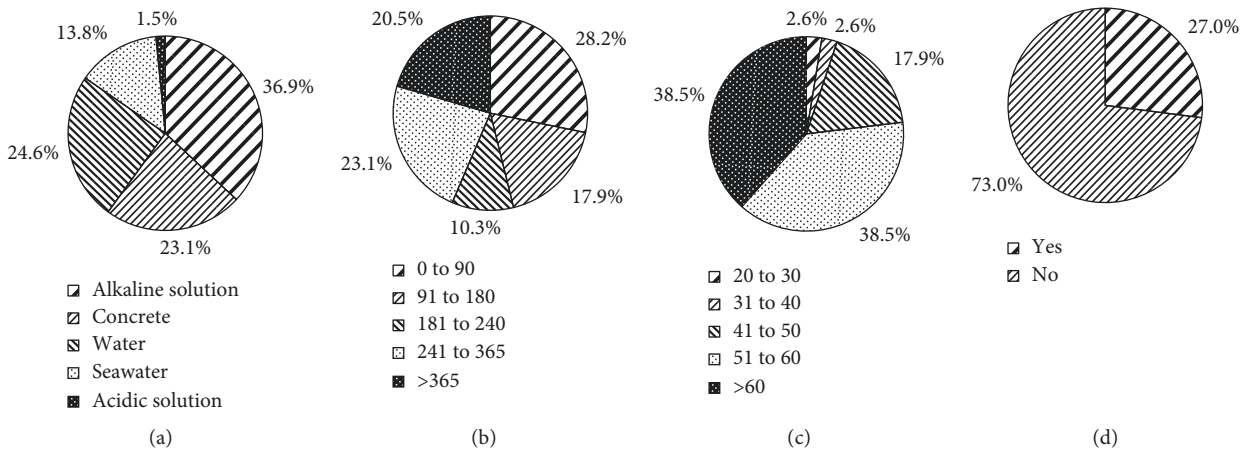

Figure 6: Percentage distribution of conditioning parameters. (a) Surrounding media. (b) Maximum conditioning duration (days). (c) Maximum conditioning temperature (°C). (d) Presence of sustained loading.

inappropriate and required revision through further research data.

3.5. Reduction Factors. The effects of service time, relative humidity, and temperature are incorporated into an environmental reduction factor for GFRP bars used as internal reinforcement in concrete structures. ACI 440.1R [2] relates the design (f^*_{fu}) and guaranteed tensile strength (f_{fu}) using the proposed reduction factors (C_E). The relationship is shown as Eq. (4). The reduction factors for environmental conditions, shown in Table 6, ranged between 0.3 and 1.0. Lower values were associated with higher relative humidity, service time, and temperature, while a reduction factor of 1 was typically attributed to less severe conditioning [61]. Another load reduction factor was introduced by several researchers and codes to account for the presence of a sustained load [2, 4, 58–60]. Its value ranged between 0.2 and 1.0, with more recent codes suggesting lower reduction factors. This is associated to the wide variations of results reported and somewhat concerning impact of accelerated aging, even though extensive research has been conducted in this area. The combined effect of both factors has also been noted, as shown in the last column of Table 6, to vary between 0.13 and 0.50.

$$f_{\mathrm{fu}} = C_{\mathrm{E}} \cdot f^*_{\mathrm{fu}}. \tag{4}$$

4. Microstructure Evaluation Methods

Microstructural characterization was employed to evaluate changes to GFRP reinforcing bars after conditioning and provide explanations to the degradation in mechanical properties. Of the many procedures available, TGA, SEM, FTIR, and DSC have been the most commonly used. Table 7 summarizes the types of microstructure tests conducted in each of the studies presented herein. While moisture uptake is not a typical microstructure evaluation method, it has been proven pivotal in understanding the causes of degradation in the properties of GFRP specimens [10]. Clearly, SEM has been the most utilized of all tests. In fact, it has been employed in 92% of the studies reviewed, while DSC, FTIR, and moisture uptake have been used in only 40–43%, as shown in Figure 7. This is mainly due to SEM being able to highlight and identify morphological changes due to conditioning, which are typically characterized by matrix degradation, interfacial deterioration, and/or fiber etching. TGA, on the other hand, has been used in 5% of the studies reviewed herein. Its primary use was to determine the thermal degradation of the polymer matrix [12, 25]. Nevertheless, it is worth noting that the majority of researchers have resorted to more than one microstructure test to confirm experimental results and findings. It should also be noted that the results reported hereafter for conditioned samples are associated to the most severe conditioning scheme utilized in each study.

4.1. Moisture Uptake. Moisture penetrates into a composite material by the flow of solution into the microgaps between polymer chains, capillary transport through fiber/matrix interfacial microcracks, and in microcracks formed during manufacturing [5]. The diffusion process mainly depends on the type of matrix and surrounding environment. It can be measured as per the procedure of ASTM D570 [20]. Typical moisture absorption/uptake tests involve weighing samples before and after immersion. However, the hydrolysis reaction that may have occurred during conditioning could cause mass dissolution and, thus, affect the results. To account for this mass loss, samples are oven-dried for 24 hours at 100°C. This oven-dried mass would then be used to find the moisture uptake:

$$\begin{aligned}&\text{moisture uptake (\%, by mass)}\\ &\quad = \frac{(\text{conditioned mass} - \text{oven dried mass})}{(\text{initial mass})} \times 100.\end{aligned} \tag{5}$$

Figure 8 is a typical moisture uptake curve that presents the increase in mass over conditioning time. Clearly, the diffusion rate of moisture is different for temperatures below

Table 6: Summary of reduction factors for GFRP reinforcing bars.

Reference	Country	Year	Reduction factor		
			Environmental	Creep/sustained load	Combined
ACI 440.1R [2]	USA	2015	0.7–0.8	0.2	0.14–0.16
FIB [4]	UK	1999	0.72	0.3	0.216
Ali, et al. [23]	Canada	2018	0.75–1.00	—	—
JSCE [57]	Japan	1997	0.77	—	—
CSA S6 [58]	Canada	2006	0.55	0.25	0.1375
NS 3473 [59]	Norway	1998	0.5	0.80–1.00	0.40–0.50
CSA S806 [60]	Canada	2012	0.75	0.3	0.225
Huang and Aboutaha [61]	USA	2010	0.31–1.00	—	—

Table 7: Summary of microstructure tests conducted on GFRP reinforcing bars.

Reference	Microstructure tests				
	Moisture uptake	TGA	SEM	FTIR	DSC
[7]	x				
[8]	x		x	x	x
[9]	x		x	x	
[10]			x	x	x
[11]	x		x	x	x
[12]	x	x	x		
[13]			x		
[14]			x	x	x
[23]	x		x	x	
[42]	x		x		
[24]	x			x	
[25]		x	x		x
[26]			x	x	x
[27]			x	x	x
[28]			x		
[29]			x		
[30]			x		
[31]	x		x	x	x
[32]			x		
[33]			x		
[34]	x		x	x	x
[35]			x	x	x
[36]			x		
[37]			x		
[38]			x	x	x
[39]	x		x	x	
[40]	x			x	
[44]			x		
[45]			x		
[46]	x		x		
[47]			x		
[48]	x			x	x
[49]			x		
[50]			x		
[51]			x		

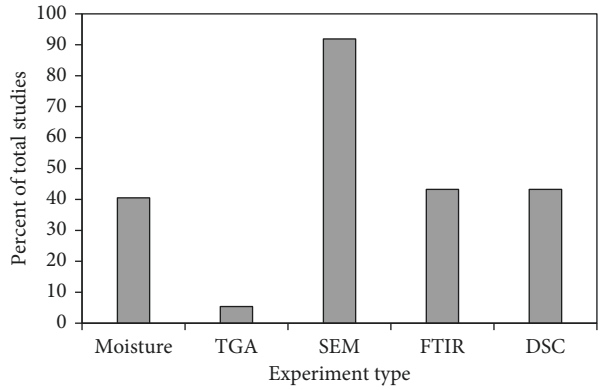

Figure 7: Percentage distribution of microstructure tests across investigated past research.

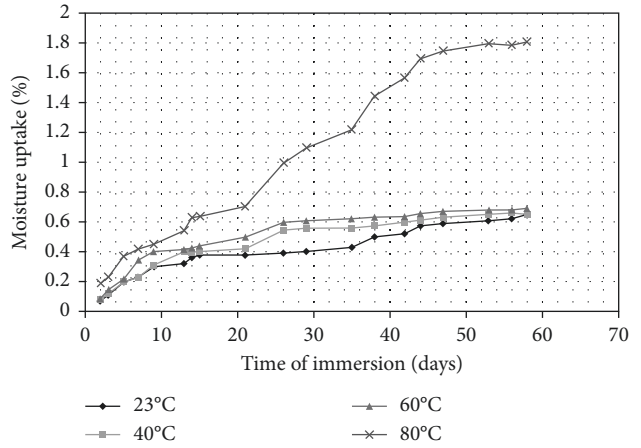

Figure 8: Typical moisture uptake curve of GFRP bars (adapted from [7]).

and above 60°C. At temperatures of 60°C and below, the majority of the uptake occurs within the first 30 days of immersion. At higher temperatures, the uptake increases at a steady rate up to 50 days. Robert, et al. [7] explained that such behavior is owed to the amplification of thermo-mechanical degradation mechanisms at a temperature of 80°C. Further, the moisture uptakes for conditioned and unconditioned GFRP reinforcing bars tested in the past literature are summarized in Table 8. These values correspond to the most severe conditioning regime employed in each study. Results for conditioned samples ranged between 0.06 and 5.1, with vinylester-GFRP presenting the widest variations. Past researchers have discussed several factors that affected the uptake, namely, presence of a sustained load, void content, pH of conditioning medium, conditioning duration, and conditioning temperature [8–11, 24, 30, 32, 35, 38, 47, 56, 64, 65]. Each factor will be discussed in the sections below.

Table 8: Results of moisture uptake of GFRP reinforcing bars.

Reference	Unconditioned		Conditioned				Within high durability limits	
	Uptake (%)	Medium	Temperature (°C)	Time (days)	Sustained load	Uptake (%)	ACI 440.6 [62]	CSA S807 [63]
[7]	0.10	Water	80	58		1.80	Not Acceptable	Not Acceptable
[8]	0.23–1.15	Alkaline	50	21		0.25–1.36	Not Acceptable	Not Acceptable
[9]	0.00	Concrete	50	Saturation		0.44	Acceptable	Acceptable
[10]	0.10	Concrete	60	450		1.23–1.50	Not Acceptable	Not Acceptable
[11]	0.10	Concrete	60	288 & 372	x	1.95–2.54	Not Acceptable	Not Acceptable
[12]	0.05	Concrete	60	48.2	x	0.50	Acceptable	Acceptable
[23]	0.23–1.15	Alkaline	60	208.3		0.25–1.36	Not Acceptable	Not Acceptable
[42]	0.00	Seawater	65	365		5.10	Not Acceptable	Not Acceptable
[24]	0.02–0.15	Water	23	Saturation		0.20	Acceptable	Acceptable
[27]	0.05–1.59	Alkaline	50	21		0.06–1.63	Not Acceptable	Not Acceptable
[32]	0.01	Alkaline	60	720		0.74	Acceptable	Not Acceptable
[35]	0.37	Concrete	50	30	x	0.57	Acceptable	Acceptable
[40]	0.40	Alkaline	50	94		1.20	Not Acceptable	Not Acceptable
[44]	0.00	Alkaline	22	16.67		0.55	Acceptable	Acceptable
[46]	0.00	Alkaline	60	360.4	x	1.10	Not Acceptable	Not Acceptable
[48]	0.01	Alkaline	60	176		0.38	Acceptable	Acceptable

The effect of sustained load can be noted by comparing the results of [10, 11]. The only difference between these two researches is the addition of a sustained load of 25% UTS in [11]. Results, presented in Table 8, show that even with an average 26% shorter conditioning durations, the uptake was, on average, 68% higher. It is thus obvious that the addition of a sustained load can aggravate the moisture uptake.

Recent work by El-Hassan, et al. [10] compared two types of GFRP bars under similar exposure conditions. The void contents were measured as 0.10 and 0.23%. The authors reported higher moisture uptake in the latter GFRP bar with higher void content. However, with limited information on the void content or fiber content in the existing literature, it is difficult to create a general conclusion. Further work would be needed to investigate the effect of void content on performance retention and microstructure changes.

To simulate severe environments, researchers have utilized alkaline solutions with different pH. Values of pH ranged between 12 and 13.6. A recent study by D'Antino, et al. [66] reported that higher pH resulted in less tensile strength retention. Yet, immersion in simulated concrete pore (alkaline) solution is not a proper reproduction of real-life concrete. The main difference is the degree of contact of alkaline solution with the GFRP reinforcing bars. In the former case, the surface of the bar is entirely coated by the solution, resulting in maximum contact area, while in the latter case, alkaline solutions remain in the concrete pores, causing limited contact with the imbedded GFRP bar. In the case of moist concrete, representing underwater concrete, the degree of contact is intermediary between the dry concrete and wet alkaline solution.

Conditioning temperature and duration have been widely investigated. Figure 8 shows the effect of each of these conditions on the moisture uptake. It is clear that higher temperatures and longer exposure durations resulted in more uptake. Yet, it is worth noting that the former was the more influential factor of the two, thus, causing a more exacerbated degradation phenomenon. Robert, et al. [7] concluded that a thermomechanical degradation mechanism would occur at an elevated temperature of 80°C, owing to higher solution diffusion in a more porous resin matrix. Nevertheless, such conditioning temperature does not correspond to service life conditions of GFRP bars, justifying the maximum aging temperature recommended by ACI 440.3 [3] and CSA S806 [60] being 60°C.

ACI 440.6 [62] and CSA S807 [63] propose durability limits in the form of maximum allowable moisture/water uptake. These limits are 1 and 0.75%, by mass, respectively, regardless of the exposure conditions. Table 8 shows the comparison of conditioned GFRP reinforcing bars with each limit. It is clear that more than half of the bars tested were not classified of high durability, based on moisture uptake. In fact, Figure 9 shows that 56 and 62% of bars, tested under the worst conditions in each study, failed to fall within the high durability limits of ACI 440.6 [62] and CSA S807 [63], respectively. In general, samples conditioned in alkaline solution at temperatures beyond 50°C were deemed unacceptable [8, 23, 27, 39, 46]. GFRP bars imbedded in concrete resulted in uptakes within the acceptable range, except for El-Hassan, et al. [11], where a sustained load of 25% UTS was applied, which is higher than the maximum allowable load recommended by ACI 440.1R [2]. A general comparison between alkaline and concrete conditioned GFRPs shows higher uptake in the former case and lower degree of satisfactoriness by the codes. Therefore, it should be noted that the moisture uptake of GFRP bars fell within the acceptable limits if conditioned in concrete and for shorter durations, lower temperatures, and/or without a sustained load. Nevertheless, in real-life scenarios, where GFRP bars are imbedded in concrete, it is possible to limit the moisture uptake by creating an impermeable concrete. This can be achieved by adding supplementary cementitious materials, as fly ash, ground granulated blast furnace slag, silica fume, or others.

4.2. TG Analysis. TG analysis was employed in the past literature to assess the decomposition of the polymer matrix

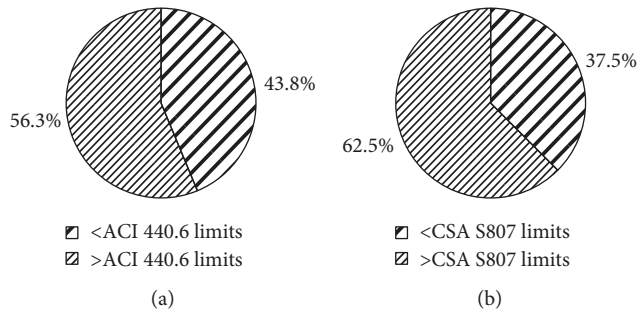

Figure 9: Percentage of GFRPs within acceptable durability limits. (a) ACI 440.6. (b) CSA S807.

under heat exposure. ASTM E1868 [19] was used to examine the change in mass as a function of temperature (20°C–800°C) and evaluate the thermal stability of the matrix. A typical mass variation curve as a function of temperature measured by TGA is shown in Figure 10. It is clear that a major mass loss of 18% occurred in the range of 300°C–450°C. This is attributed to the thermal degradation of the polymer matrix, as the molecular chains broke, leading to microcrack formation at the fiber/matrix interface and matrix itself. Such mass loss also indicates a critical loss of mechanical properties due to an irreversible degradation mechanism.

4.3. FTIR Analysis. A number of past studies explored the degradation mechanism of GFRP reinforcing bars using FTIR analysis. Samples were placed in an FTIR spectrometer and analysed from 400 to 4000 cm^{-1} in transmittance or absorbance mode. Figure 11 shows typical FTIR spectra for conditioned and unconditioned samples. Five zones could be identified: 900–1200, 1400–1600, 1600–1800, 2800–3100, and 3200–3600 cm^{-1}. These spectral zones are, respectively, attributed to O–H bending, C–O stretching, C=O stretching, C–H stretching, and O–H stretching. The past literature studies have identified and reported these peaks, as shown in Table 9. It is clear that most conducted research has focused on the O–H and C–H stretching bonds. This is owed to the ability to evaluate the hydrolysis reaction by measuring the peak in the OH band, which increases due to hydrolysis and relating it to the constant peak of CH. As such, the relative quantity of hydroxyl groups is characterized by the ratio of maximum peaks of OH-to-CH [13, 14, 27, 34]. Table 10 presents the OH-to-CH ratio of conditioned and control specimens of numerous studies. It should be noted that the reported ratio for conditioned samples is a result of the most severe conditioning scheme utilized in each study. This is a typical approach adopted by several researchers [8, 9, 13, 14, 24, 26, 31, 34]. The ratio for control GFRP bars ranged between 0.21 and 2.60, while that of conditioned counterparts was between 0.25 and 14.30. With such wide variations in the degradation, i.e., OH-to-CH ratio, the percentage increase was calculated and reported in Table 10. It ranged between 0 and 450%. Thus, to provide a more conclusive interpretation of the results, a more isolated investigation is performed. GFRP bars made with epoxy and vinylester are separated and each correlated to its associated moisture

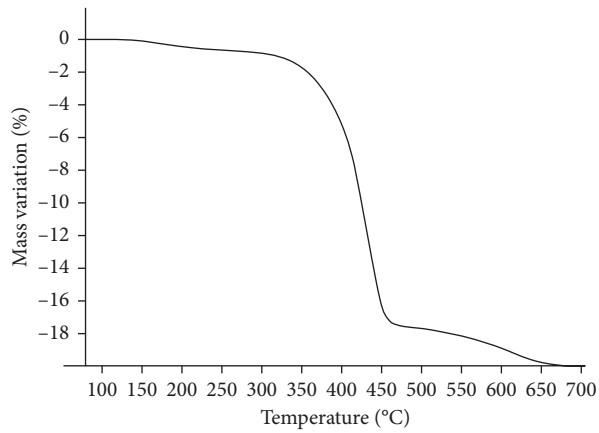

Figure 10: Mass variation of GFRP bar specimen when heated between 20°C and 800°C (adapted from [25]).

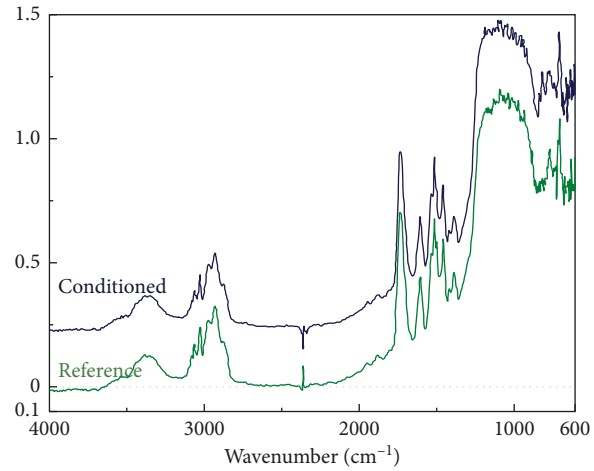

Figure 11: Glass transition temperature of conditioned and reference GFRP bars (adapted from [24]).

uptake. Results of Figure 12(a) show that the higher the moisture uptake, the higher the OH/CH increase due to conditioning of epoxy-GFRP bars. These test samples were all conditioned at 60°C, but for different durations. In fact, the left marker (0.74% moisture uptake increase) was conditioned in alkaline solution for up to 720 days, but did not show any increase in OH/CH ratio, indicating no degradation due to hydrolysis reaction [31]. This shows that

Table 9: Summary of FTIR wavelengths detected in conditioned GFRP reinforcing bars.

Reference	Wavelength (cm^{-1})				
	O–H stretch	C=O stretch	C–H stretch	C–O stretch	O–H bend
[8]	3200–3650	—	2800–3000	—	—
[9]	3300–3600	1600–1800	2800–3100	1400–1600	900–1100
[10]	3200–3600	—	2800–3000	—	—
[11]	3200–3600	—	2800–3000	—	—
[13]	3300–3600	—	2800–3100	—	—
[14]	3300–3600	—	2800–3000	—	—
[23]	3200–3650	—	2800–3000	—	—
[24]	3300–3600	1600–1800	2800–3100	1400–1600	900–1200
[26]	3200–3500	—	2800–3000	—	—
[27]	3300–3600	—	2850–3100	—	—
[31]	3400	—	3026	—	—
[34]	3200–3400	—	2800–3100	—	—
[35]	3430	—	2900	—	—
[38]	3430	—	2900	—	—
[39]	3540	—	2900	—	—
[40]	3334	1557	2900	1420	1019

Table 10: Results of OH/CH ratios in control and conditioned GFRP reinforcing bars.

Reference	Resin type	Conditioning				OH/CH		
		Medium	Temperature (°C)	Time (days)	Sustained load	Control	Conditioned	% Increase
[8]	Polyester	Alkaline	60	208.3		2.6 & 1.6	14.3 & 3.5	450 & 118.8
[9]	Vinylester	Concrete	50	60		No change		—
[10]	Epoxy	Concrete	60	450		0.59 & 1.07	1.15 & 1.24	94.9 & 15.9
[11]	Epoxy	Concrete	60	288 & 372	x	0.59 & 1.07	1.27 & 1.27	115.3 & 18.7
[13]	Vinylester	Water	50	180		0.45	0.51	13.3
[14]	Vinylester	Concrete	50	240		0.21	0.25	19.0
[23]	Polyester	Alkaline	60	208.3		2.6 & 1.6	14.3 & 3.5	450 & 118.8
[24]	Vinylester	Water	23	90		No change		—
[26]	Vinylester	Alkaline	70	365		No change		—
[27]	Vinylester polyester	Alkaline	60	180		0.49 & 0.48	0.54 & 0.87	22.7 & 81.3
[31]	Epoxy	Alkaline	60	720		No change		—
[34]	Vinylester	Concrete	50	30	x	0.51	0.53	3.9
[35]	Vinylester	Alkaline	73	120	x	1.05	1.45 & 1.30	38.1 & 23.8
[38]	Vinylester	Concrete	30	2920	x	No change		—
[39]	Vinylester	Alkaline	50	365		1.05	1.18	12.4
[40]	Vinylester	Alkaline	22	16.67		No change		—

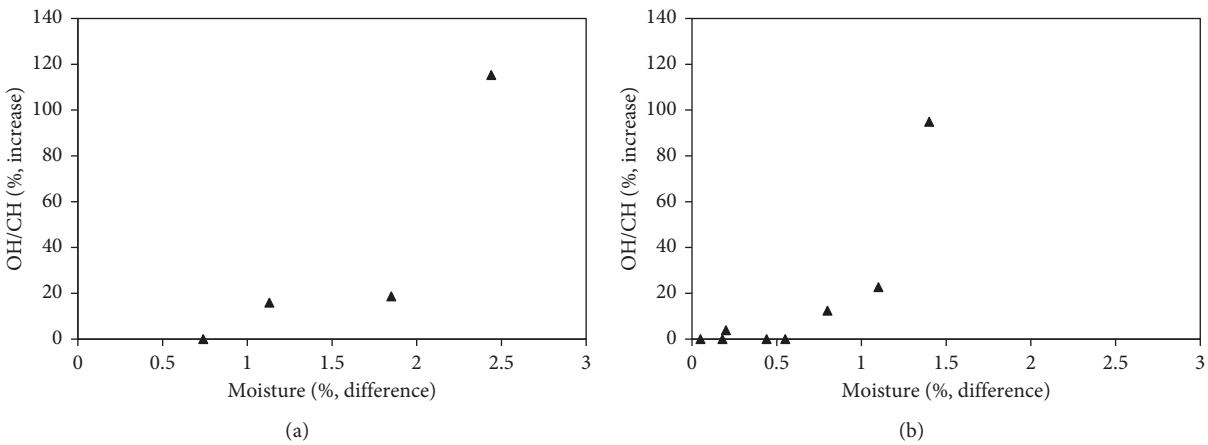

Figure 12: Correlation between OH/CH increase (%) and moisture uptake due to conditioning (%). (a) GFRP with epoxy matrix. (b) GFRP with vinylester matrix.

the degradation only initiated after 1% moisture uptake. Further increase in uptake up to 2% did not cause significant impact on the change in OH/CH ratio, after which it dramatically increased up to 115%. Thus, it can be concluded that epoxy-GFRP bars could experience limited degradation if the moisture uptake is maintained below 2%, by mass.

Figure 12(b) presents a relation between OH/CH percent increase and moisture uptake in conditioned GFRP bars made with vinylester matrix. The OH/CH increase remained below 20%, indicating a lower degree of hydrolysis reaction, when the moisture uptake was below 1.5%. Beyond 1.5%, degradation was much more significant due to conditioning, with OH/CH increasing by up to 95% compared to the control samples. In comparison and based on the studies revised in this paper, GFRP bars made with vinylester resin have been found to be more generally susceptible to hydrolysis than their epoxy counterparts.

The effect of the initial tensile strength of unconditioned GFRP bars on their resistance to degradation was investigated in [10, 11]. In these studies, two different types of GFRP bars with dissimilar tensile strengths were compared. FTIR analysis results of [10], presented in Table 10, show that the GFRP bar with lower void content had an increase in OH/CH ratio of 15.9% compared to 94.9% for the sample with the higher void content. Obviously, as the void content increased, the hydrolysis reaction progressed, leading to higher OH/CH ratios. The degradation was further intensified upon the application of a sustained load, as shown in the results of [11].

4.4. DSC Analysis. The thermal behavior and characteristics of conditioned and control GFRP samples is analysed using DSC. The main properties obtained from DSC are glass transition temperature (T_g), curing process, melting temperature, crystallinity, relaxation, and thermal stability [25]. Of these properties, glass transition temperature is the most reported in the past literatures. It is determined by performing two scans, each from 20°C to 250°C, in accordance with ASTM E1356 [21]. The first scan compares the T_g of the conditioned and control samples. A reduction in T_g is indicative of matrix plasticization. The second scan identifies the degradation mechanism, whereby a similar T_g for conditioned and control samples indicates a reversible plasticizing effect, while a lower T_g for the former signifies an irreversible chemical degradation. Figure 13 illustrates typical DSC curves for alkaline-conditioned and unconditioned GFRP reinforcing bars. The step shown in the range of 90°C–110°C is used to find the T_g. While it appeared to be an endothermic or melting peak, there was no melting involved in this work [31]. In fact, the authors associated this peak to "the thermal stress relaxation phenomenon of polymer chains of the GFRP rebar during long-term ageing".

Furthermore, a summary of T_g temperatures and cure ratio of various studies is presented in Table 11. These temperatures are results of the GFRP samples subject to the most severe conditioning scheme utilized in each study. It is clear that most studies experienced some decrease in the T_g of the first scan, ranging from 0 to 46%. This wide variation

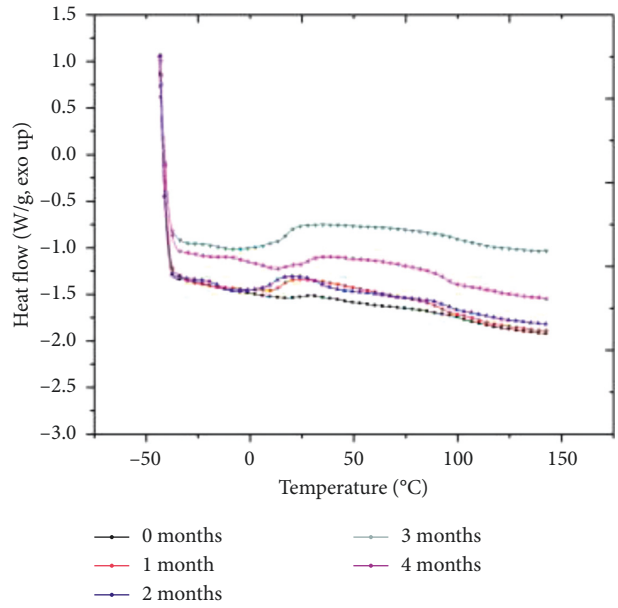

Figure 13: Differential scanning calorimetry curve for conditioned and control GFRP bars (adapted from [31]).

in results is owed to the different curing regimes, fiber content, matrix type, and presence of sustained loading, which all contribute to lowering the T_g and the deterioration of the GFRP bars. However, it is possible to isolate some values by selecting GFRP bars made with epoxy matrix and correlating them to other parameters. Figure 14 shows that higher changes in OH/CH ratios led to more intense reductions in the T_g. This shows a clear correlation between results of FTIR and DSC, signifying the progression of a hydrolysis reaction. In other terms, the factors that affect the OH/CH ratios have a similar effect on the T_g.

In the second scan, studies that employed concrete as the conditioning medium did not note any change in the T_g between conditioned and control samples [10, 11, 14, 34, 38]. On the other hand, specimens conditioned in alkaline solutions and water showed some signs of irreversible chemical degradation, with the former conditioning scheme being more detrimental [25, 27, 42]. This provides evidence to the severity of conditioning in alkaline solutions, rendering results somewhat unrealistic and unreliable.

Additionally, the cure ratio is shown in Table 11. It is the ratio of the T_g of the first to second scan for the control samples. Other than [13, 14, 34], which are conducted by the same authors and probably using the same GFRP bars, the reported cure ratios were above 95%. Lower values signify that the samples were not fully cured and that postcuring occurred during the second scan.

4.5. SEM Analysis. SEM was employed to evaluate the microstructure and morphological changes to the GFRP reinforcing bars after conditioning. The fiber-matrix interface is considered one of the most vulnerable areas in GFRP reinforcing bars. It is merely a few microns thick and plays a critical role in transfer of the load between fiber and

Table 11: Results of T_g temperatures and cure ratio in control and conditioned GFRP reinforcing bars.

Reference	T_g						Cure ratio (%)
	1st scan (°C)			2nd scan (°C)			
	Control	Conditioned	Decrease (%)	Control	Conditioned	Decrease (%)	
[8]	93, 113, 126	98, 100, 112	5.4, 11.5, 11.1	—	—	—	98–100
[9]	145	140	3.4	—	—	—	—
[10]	101 & 125	95 & 90	5.9 & 28	106 & 125	105 & 126	0.0	95.3 & 100
[11]	101 & 125	90 & 90	10.9 & 28	106 & 125	105 & 125	—	95.3 & 100
[13]	110	103	6.4	129	128	0.8	85.3
[14]	105	104	1.0	134	129	3.7	78.4
[42]	116	62	46.6	120	83	30.8	96.7
[24]	105–125	—	—	105–125	—	—	100.0
[25]	112	67	40.2	113	68	39.8	99.1
[26]	116	117	—	117	118	—	99.1
[27]	123, 124, 90	122, 123, 84	0, 0, 6.6	124, 123, 90	123, 122, 85	0, 0, 5.5	100
[31]	105	96	8.6	—	—	—	—
[34]	112	95	15.2	131	130	0.8	85.5
[35]	114	105	7.9	120	120	0.0	95.0
[38]	124	120	3.2	125	120	4.0	99.2
[48]	115–125	112–124	2.4–2.6	—	—	—	—

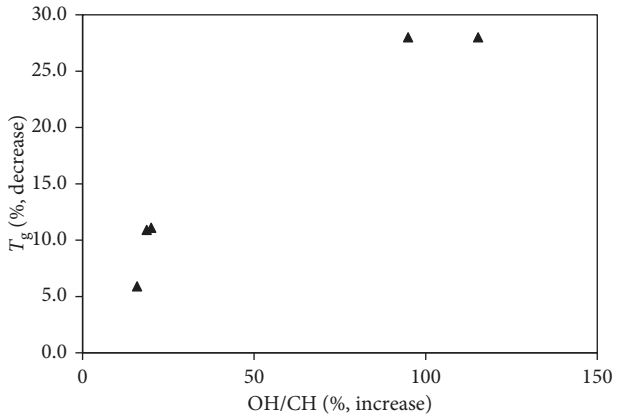

Figure 14: Percent increase of T_g of the first scan as a function of percent increase of OH/CH after conditioning of epoxy-GFRP bars.

matrix [67]. In the presence of moisture and alkalis, the bond between fiber and matrix is weakened, causing damage to the interface itself and the GFRP as a whole.

Micrographs typically highlight different damages or deteriorations that may be induced by conditioning, including matrix degradation, fiber/material interface degradation, microcrack formation, and fiber etching and leaching. Table 12 shows a summary of deteriorations that have been identified in different studies using SEM. Clearly, matrix degradation, fiber/matrix interfacial degradation, and microcrack formation are interlinked, as they are reported simultaneously in multiple studies; they are denoted collectively hereafter as damage A. Fiber etching and leaching, on the other hand, is designated as damage B. Of the literature reviewed in this work, 58, 15, and 27% reported damage A, damage B, and no damage, respectively, as shown in Figure 15. This demonstrates that the matrix and the fiber/matrix interface are indeed the most vulnerable components of GFRP reinforcing bars, with much lesser deterioration of the fiber.

Figure 16(a) shows a micrograph from past work that identified damage A in a conditioned GFRP reinforcing bar [10]. Samples in this study were placed in seawater-contaminated concrete for 15 months at 60°C. Clearly, the fiber/matrix interface weakened to the extent that fiber delamination occurred. This is primarily owed to the progression of hydrolysis reaction.

Fiber etching and leaching were only noticed in research work that examined the durability performance of GFRP reinforcing bars made with E-glass/vinylester and conditioned in alkaline environment; they are represented as damage B. Figure 16(b) presents a micrograph of a GFRP bar that suffered damage B [28] with circumferential damage to the fiber. In this work, GFRP samples were conditioned in an alkaline solution under a 25% UTS sustained load. The severity of the testing conditions resulted in all samples failing within 20 days of conditioning. No tensile strength could be retained at that point. The degree of deterioration was too harsh that it caused matrix degradation, fiber/matrix interfacial debonding, microcrack formation, and fiber damage simultaneously.

In some of the reviewed studies, no damage or deterioration was noticed. Though some degradation may have been reported in the microstructure study, the mechanical properties of GFRP reinforcing bars were not significantly affected. It is thus critical for researchers to correlate the tensile strength, moisture uptake, OH/CH ratio, and SEM micrographs in a distinct study to provide a better understanding of the effect of the microstructure on the mechanical properties. Yet, while the scope of this work is to focus on microstructure characteristics of GFRP bars exposed to different conditioning regimes, a correlation based on the reviewed studies has been developed. For this matter, results from [10, 11, 13, 14, 27, 35] are employed. It is worth noting the GFRP samples were conditioned differently in these studies. The SEM micrographs of Figures 17(a)–17(f) show little to no cracks at the fiber/matrix interface, indicating limited degradation. The GFRPs of [10, 11, 27] are

Table 12: Summary of deteriorations identified by SEM in conditioned GFRP reinforcing bars.

Reference	Deterioration/Damages			
	Matrix degradation	Fiber/matrix interface damage	Microcracks	Fiber etching and leaching
[8]	x	x	x	
[9]	No deterioration reported			
[10]	x	x	x	
[11]	x	x	x	
[12]	x	x	x	
[13]	No deterioration reported			
[14]	No deterioration reported			
[15]	x	x	x	x
[23]	x	x	x	
[42]	x	x		
[24]	No deterioration reported			
[25]	x	x	x	
[26]	No deterioration reported			
[27]	x	x	x	
[28]	x	x	x	x
[29]	x	x	x	
[30]	x	x	x	
[31]	No deterioration reported			
[32]	x	x	x	
[33]	x	x	x	
[34]	No deterioration reported			
[35]	x	x	x	
[36]	x	x	x	x
[37]	x	x	x	
[38]	No deterioration reported			
[39]	x	x	x	
[44]	x	x	x	
[45]	x	x	x	
[46]	x	x	x	x
[47]	x	x	x	
[49]	x	x	x	
[50]	x	x	x	x
[51]	No deterioration reported			

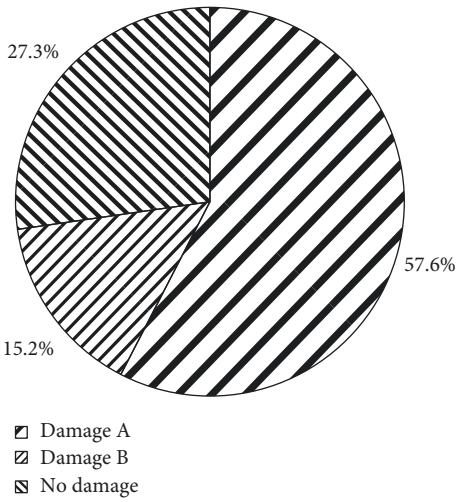

Figure 15: Distribution of damage/deterioration in conditioned GFRP reinforcing bars.

associated with moisture uptakes of 1.20, 1.95, and 1.63%, respectively. The respective increases in OH/CH ratios of [10, 11, 13, 14, 27, 35] are 15.9, 18.5, 13.3, 19.0, 22.7, and 3.9%. The strength retention of these samples was 85, 73, 93, 84, 100, and 84%, respectively. Yet, samples in [11, 35] were conditioned under sustained loads. Accordingly, it is possible to accept an increase in moisture uptake and OH/CH ratio up to a threshold of 1.6 and 18%, respectively, while anticipating up to 15% reduction in tensile strength.

5. Conclusions and Remarks

In this paper, studies examining the microstructure of GFRP reinforcing bars exposed to different environmental conditions and sustained loading were reviewed. Experimental results and findings were collected from past literature, analysed, and compared to provide conclusive remarks on the effect of conditioning on the microstructure of GFRP reinforcing bars. Based on the conducted analysis, the following conclusions can be drawn:

(i) Mechanical properties from the past literature were used to provide correlation equations for unconditioned GFRP bars. Tensile strength and modulus of as-received GFRP bars were correlated in a linear equation. These relationships could

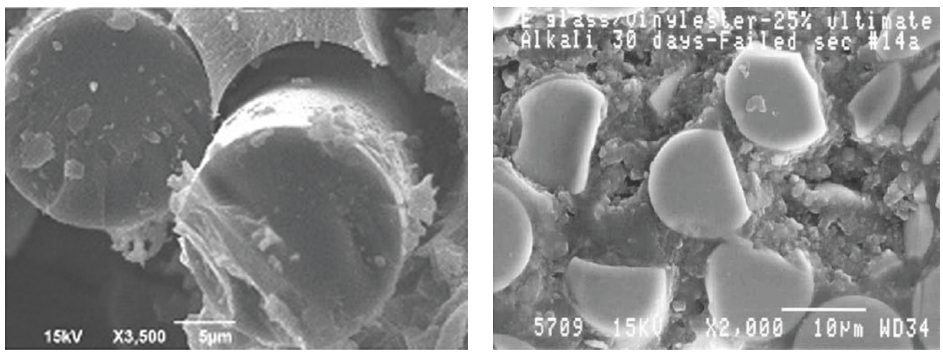

(a) (b)

Figure 16: Micrograph of conditioned GFRP reinforcing bar. (a) Damage A (adapted from [10]). (b) Damage B (adapted from [28]).

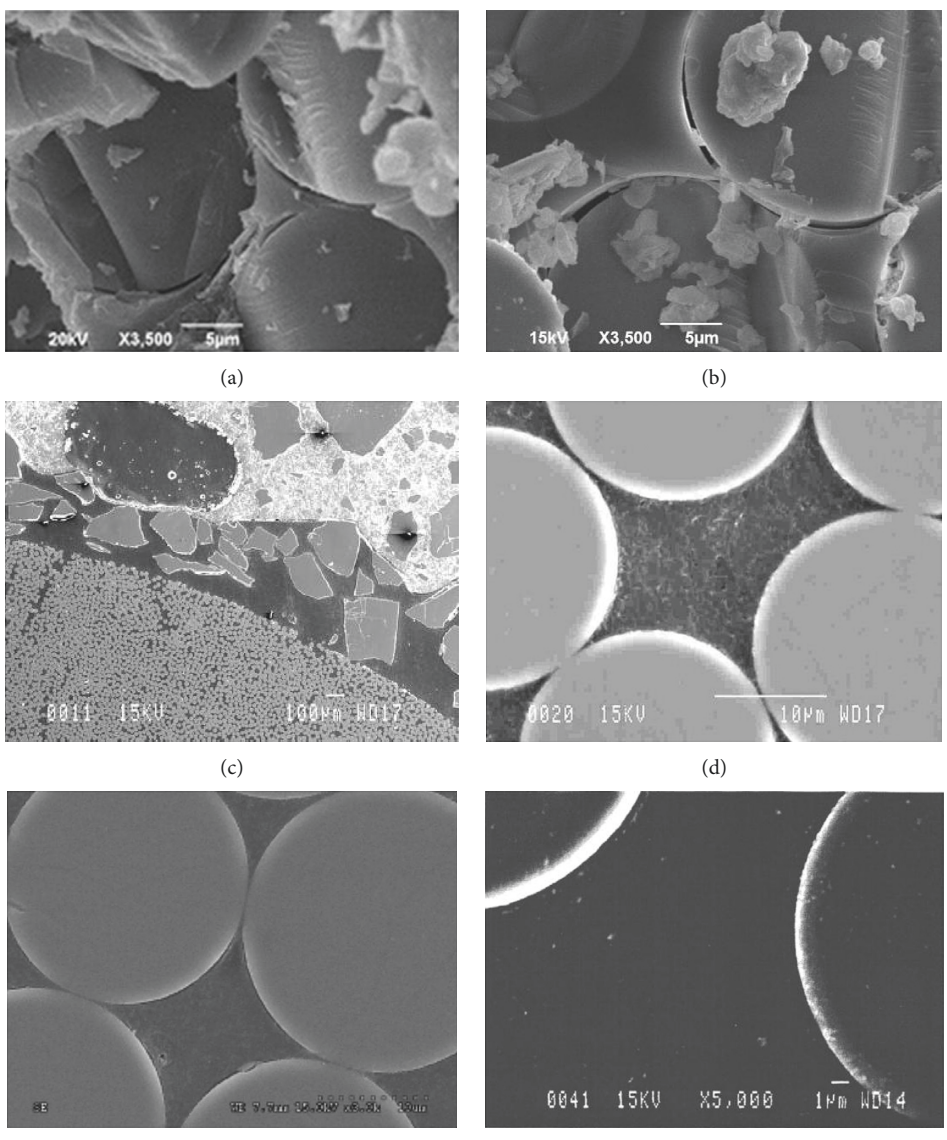

(a) (b)

(c) (d)

(e) (f)

Figure 17: Micrograph of conditioned GFRP reinforcing bar with no damage. (a) Adapted from [10]. (b) Adapted from [11]. (c) Adapted from [13]. (d) Adapted from [14]. (e) Adapted from [27]. (f) Adapted from [35].

provide reasonably accurate prediction of the tensile modulus from the tensile strength.

(ii) Only 14% of reviewed studies investigated the performance and microstructure of GFRP bars made with E-glass and epoxy. On average, the tensile properties of such unconditioned bars seemed to be 14% superior to those of vinylester counterparts. Discrepancies in the testing procedures did not allow for a direct microstructure comparison between the two types. Further testing is needed prior to the adoption of these GFRP reinforcing bars.

(iii) In the majority of reviewed studies, GFRP specimens were conditioned in alkaline and water solutions due to the ease of the experimental setup. Concrete was only employed in 23% of the studies. Conditioning durations varied greatly, with 0–90 and more than 365 days being most commonly used.

(iv) The application of a sustained load to GFRP reinforcing bars during conditioning was adopted in 28% of the studies reviewed. Research studies that exceeded the limits stated by codes and standards concluded that the set limits were only valid for specific nonaggressive environment conditions. In fact, elevated temperatures promoted the degradation mechanism. More research is needed to update these limits to include different conditioning regimes.

(v) Higher temperature, prolonged conditioning, presence of a sustained load, and conditioning in alkaline solution caused an increase in moisture uptake. Most uptake values extracted from the literature exceeded the limits set by ACI 440.6 [62] and CSA S807 [63]. Only specimens that were conditioned in concrete at low temperatures, for short durations, and/or without a sustained load were within the acceptable moisture uptake durability limits. This raises a concern to the aggressiveness of the conditioning utilized in the literature.

(vi) A correlation was developed between the progression of hydrolysis (OH/CH increase) and the decrease in T_g (%). Within an increase of 20% OH/CH, the T_g decreased by only 10%. However, greater surges in OH/CH caused much more dramatic reductions in the glass transition temperature. Nevertheless, limiting the moisture uptake could control the increase in hydroxyl groups.

(vii) Conditioning in alkaline solution was found to be too severe and did not accurately represent real-life scenarios. Specimens conditioned in alkaline solutions experienced irreversible chemical degradation, more hydroxyl group formation, and more intense degradation to the microstructure.

(viii) Four types of damages were reported in conditioned GFRP bars: matrix degradation, fiber degradation, fiber/matrix interface degradation, and microcrack formation. Most of concrete-encased GFRP specimens did not experience excessive degradation, as opposed to alkaline conditioning that severely damaged the GFRP.

(ix) The increase in moisture uptake and OH/CH ratio and formation of microcracks does not necessarily have a severe effect on the mechanical performance. In fact, it is possible to allow an increase in moisture uptake and OH/CH ratio up to 1.6 and 18%, respectively, while anticipating up to 15% reductions in tensile strength.

The conclusions presented above were based on the past literature reviewed in this work. Further studies are needed to fill the research gaps before GFRP reinforcing bars could be widely adopted by the construction industry. The following are suggestions for future research direction:

(i) A standard testing procedure for GFRP reinforcing bars capable of providing consistent and reliable results that represents real-life scenarios

(ii) Comparative performance and microstructure evaluation of GFRP reinforcing bars in concrete and subjected to different environment conditions and levels of sustained load

(iii) Microstructure characterization of GFRP bars exposed to acidic solution

(iv) The effect of void content on performance retention and microstructure changes of GFRP reinforcing bars

(v) Performance and microstructure comparison between GFRP bars made with different resin, i.e., epoxy and vinylester, subject to the same conditioning schemes

(vi) Performance and microstructure comparison between concrete-encased GFRP specimens exposed to elevated temperatures with an applied sustained load and actual in-service specimens

(vii) GFRP reinforcing bars in concretes made with different supplementary cementitious materials to limit the moisture uptake

Conflicts of Interest

The authors declare that there are no conflicts of interest regarding the publication of this paper.

Acknowledgments

This research publication is supported by the Abu Dhabi Department of Education and Knowledge (ADEK) and United Arab Emirates University (UAEU) under grant 21N209.

References

[1] G. Koch, "1-Cost of corrosion," in *Trends in Oil and Gas Corrosion Research and Technologies*, A. M. El-Sherik, Ed., Woodhead Publishing, Boston, MA, USA, 2017.

[2] ACI 440.1R, *Guide for the Design and Construction of Concrete Reinforced with FRP Bars*, American Concrete Institute, Farmington Hills, MI, USA, 2015.

[3] ACI 440.3R, *Guide Test Methods for Fiber-Reinforced Polymers (FRPs) for Reinforcing or Strengthening Concrete Structures*, American Concrete Institute, Farmington Hills, MI, USA, 2012.

[4] FIB, "FRP reinforcement in RC structures," in *Bulletin 40*, The International Federation for Structural Concrete FIB, Lausanne, Switzerland, 2007.

[5] H. P. Abeysinghe, W. Edwards, G. Pritchard, and G. J. Swampillai, "Degradation of crosslinked resins in water and electrolyte solutions," *Polymer*, vol. 23, no. 12, pp. 1785–1790, 1982.

[6] P. V. Vijay and H. V. S. GangaRao, "Accelerated and natural weathering of glass fiber reinforced plastic bars," in *Proceedings of the 4th International Conference on Fibre-Reinforced Plastics for Reinforced Concrete Structures*, Baltimore, MD, USA, 1999.

[7] M. Robert, P. Wang, P. Cousin, and B. Benmokrane, "Temperature as an accelerating factor for long-term durability testing of FRPS: should there be any limitations?," *Journal of Composites for Construction*, vol. 14, no. 4, pp. 361–367, 2010.

[8] B. Benmokrane, A. H. Ali, H. M. Mohamed, A. ElSafty, and A. Manalo, "Laboratory assessment and durability performance of vinyl-ester, polyester, and epoxy glass-FRP bars for concrete structures," *Composites Part B: Engineering*, vol. 114, pp. 163–174, 2017.

[9] B. Benmokrane, H. M. Mohamed, A. Manalo, and P. Cousin, "Evaluation of physical and durability characteristics of new headed glass fiber-reinforced polymer bars for concrete structures," *Journal of Composites for Construction*, vol. 21, no. 2, article 04016081, 2017.

[10] H. El-Hassan, T. El-Maaddawy, A. Al-Sallamin, and A. Al-Saidy, "Performance evaluation and microstructural characterization of GFRP bars in seawater-contaminated concrete," *Construction and Building Materials*, vol. 147, pp. 66–78, 2017.

[11] H. El-Hassan, T. El-Maaddawy, A. Al-Sallamin, and A. Al-Saidy, "Durability of glass fiber-reinforced polymer bars conditioned in moist seawater-contaminated concrete under sustained load," *Construction and Building Materials*, vol. 175, pp. 1–13, 2018.

[12] B. Benmokrane, P. Wang, T. M. Ton-That, H. Rahman, and J.-F. Robert, "Durability of glass fiber-reinforced polymer reinforcing bars in concrete environment," *Journal of Composites for Construction*, vol. 6, no. 3, pp. 143–153, 2002.

[13] M. Robert and B. Benmokrane, "Effect of aging on bond of GFRP bars embedded in concrete," *Cement and Concrete Composites*, vol. 32, no. 6, pp. 461–467, 2010.

[14] M. Robert, P. Cousin, and B. Benmokrane, "Durability of GFRP reinforcing bars embedded in moist concrete," *Journal of Composites for Construction*, vol. 13, no. 2, pp. 66–73, 2009.

[15] H. Roh, C. Park, and D. Y. Moon, "Experimental investigation of the effects of concrete alkalinity on tensile properties of preheated structural GFRP rebar," *Advances in Materials Science and Engineering*, vol. 2017, p. 13, 2017.

[16] ASTM, *Standard Test Method for Tensile Properties of Fiber Reinforced Polymer Matrix Composite Bars*, D7205, ASTM International, West Conshohocken, PA, USA, 2016.

[17] ASTM, *Standard Test Methods for Constituent Content of Composite Materials*, D3171, ASTM, West Conshohocken, PA, USA, 2015.

[18] ASTM, *Standard Test Methods for Void Content of Reinforced Plastics*, D2734, ASTM International, West Conshohocken, PA, USA, 2016.

[19] ASTM, *Standard Test Methods for Loss-On-Drying by Thermogravimetry*, E1868, ASTM, West Conshohocken, PA, USA, 2015.

[20] ASTM, *Standard Test Method for Water Absorption of Plastics*, D570, ASTM, West Conshohocken, PA, USA, 2010.

[21] ASTM, *Standard Test Method for Assignment of the Glass Transition Temperatures by Differential Scanning Calorimetry*, E1356, ASTM, West Conshohocken, PA, USA, 2008.

[22] ASTM, *Standard Test Method for Linear Thermal Expansion of Solid Materials by Thermomechanical Analysis*, E831, ASTM International, West Conshohocken, PA, USA, 2014.

[23] A. H. Ali, B. Benmokrane, H. M. Mohamed, A. Manalo, and A. El-Safty, "Statistical analysis and theoretical predictions of the tensile-strength retention of glass fiber-reinforced polymer bars based on resin type," *Journal of Composite Materials*, vol. 52, no. 21, pp. 2929–2948, 2018.

[24] B. Benmokrane, A. Manalo, J.-C. Bouhet, K. Mohamed, and M. Robert, "Effects of diameter on the durability of glass fiber-reinforced polymer bars conditioned in alkaline solution," *Journal of Composites for Construction*, vol. 21, no. 5, article 04017040, 2017.

[25] M. Robert and B. Benmokrane, "Behavior of GFRP reinforcing bars subjected to extreme temperatures," *Journal of Composites for Construction*, vol. 14, no. 4, pp. 353–360, 2010.

[26] M. Robert and B. Benmokrane, "Combined effects of saline solution and moist concrete on long-term durability of GFRP reinforcing bars," *Construction and Building Materials*, vol. 38, pp. 274–284, 2013.

[27] M. Montaigu, M. Robert, E. A. Ahmed, and B. Benmokrane, "Laboratory characterization and evaluation of durability performance of new polyester and vinylester E-glass GFRP dowels for jointed concrete pavement," *Journal of Composites for Construction*, vol. 17, no. 2, pp. 176–187, 2013.

[28] G. M. Rajan Sen and S. Tom, "Durability of E-glass/vinylester reinforcement in alkaline solution," *ACI Structural Journal*, vol. 99, no. 3, pp. 369–375, 2002.

[29] J.-P. Won and C.-G. Park, "Effect of environmental exposure on the mechanical and bonding properties of hybrid FRP reinforcing bars for concrete structures," *Journal of Composite Materials*, vol. 40, no. 12, pp. 1063–1076, 2006.

[30] Y. A. Al-Salloum, S. El-Gamal, T. H. Almusallam, S. H. Alsayed, and M. Aqel, "Effect of harsh environmental conditions on the tensile properties of GFRP bars," *Composites Part B: Engineering*, vol. 45, no. 1, pp. 835–844, 2013.

[31] M. A. Sawpan, A. A. Mamun, and P. G. Holdsworth, "Long term durability of pultruded polymer composite rebar in concrete environment," *Materials & Design*, vol. 57, pp. 616–624, 2014.

[32] S. Alsayed, Y. Al-Salloum, T. Almusallam, S. El-Gamal, and M. Aqel, "Performance of glass fiber reinforced polymer bars under elevated temperatures," *Composites Part B: Engineering*, vol. 43, no. 5, pp. 2265–2271, 2012.

[33] A. Mukherjee and S. J. Arwikar, "Performance of glass fiber-reinforced polymer reinforcing bars in tropical environments—Part II: microstructural tests," *ACI Structural Journal*, vol. 102, no. 6, pp. 816–822, 2005.

[34] M. Robert and B. Benmokrane, "Physical, mechanical, and durability characterization of preloaded GFRP reinforcing bars," *Journal of Composites for Construction*, vol. 14, no. 4, pp. 368–375, 2010.

[35] A. S. Debaiky, G. Nkurunziza, B. Benmokrane, and P. Cousin, "Residual tensile properties of GFRP reinforcing bars after loading in severe environments," *Journal of Composites for Construction*, vol. 10, no. 5, pp. 370–380, 2006.

[36] H.-Y. Kim, Y.-H. Park, Y.-J. You, and C.-K. Moon, "Short-term durability test for GFRP rods under various environmental conditions," *Composite Structures*, vol. 83, no. 1, pp. 37–47, 2009.

[37] T. H. Almusallam, Y. A. Al-Salloum, S. H. Alsayed, S. El-Gamal, and M. Aqel, "Tensile properties degradation of glass fiber-reinforced polymer bars embedded in concrete under severe laboratory and field environmental conditions," *Journal of Composite Materials*, vol. 47, no. 4, pp. 393–407, 2013.

[38] A. A. Mufti, N. Banthia, B. Benmokrane, M. Boulfiza, and J. P. Newhook, "Durability of GFRP composite rods," *Concrete International*, vol. 29, no. 2, pp. 37–42, 2007.

[39] A. S. M. Kamal and M. Boulfiza, "Durability of GFRP rebars in simulated concrete solutions under accelerated aging conditions," *Journal of Composites for Construction*, vol. 15, no. 4, pp. 473–481, 2011.

[40] J. W. Chin, K. Aouadi, M. R. Haight, W. L. Hughes, and T. Nguyen, "Effects of water, salt solution and simulated concrete pore solution on the properties of composite matrix resins used in civil engineering applications," *Polymer Composites*, vol. 22, no. 2, pp. 282–297, 2001.

[41] B. Benmokrane, F. Elgabbas, E. A. Ahmed, and P. Cousin, "Characterization and comparative durability study of glass/vinylester, basalt/vinylester, and basalt/epoxy FRP bars," *Journal of Composites for Construction*, vol. 19, no. 6, article 04015008, 2015.

[42] A.-H. I. Mourad, B. M. Abdel-Magid, T. El-Maaddawy, and M. E. Grami, "Effect of seawater and warm environment on glass/epoxy and glass/polyurethane composites," *Applied Composite Materials*, vol. 17, no. 5, pp. 557–573, 2010.

[43] ASTM, *Standard Test Method for Flexural Properties of Fiber Reinforced Pultruded Plastic Rods*, D4476, ASTM International, West Conshohocken, PA, USA, 2014.

[44] F. Micelli and A. Nanni, "Durability of FRP rods for concrete structures," *Construction and Building Materials*, vol. 18, no. 7, pp. 491–503, 2004.

[45] W. Li, C. Ji, H. Zhu, F. Xing, J. Wu, and X. Niu, "Experimental investigation on the durability of glass fiber-reinforced polymer composites containing nanocomposite," *Journal of Nanomaterials*, vol. 2013, p. 11, 2013.

[46] H. Fergani, M. Di Benedetti, M. Guadagnini, C. Lynsdale, and C. Mias, "Characterization and durability study of GFRP bars exposed to severe environments and under sustained loads," in *Proceedings of the Fifth International Conference on Durability of Fiber Reinforced Polymer (FRP) Composites for Construction and Rehabilitation of Structures*, QC, Canada, 2017.

[47] J. F. Davalos, Y. Chen, and I. Ray, "Long-term durability prediction models for GFRP bars in concrete environment," *Journal of Composite Materials*, vol. 46, no. 16, pp. 1899–1914, 2012.

[48] M. A. Sawpan, P. G. Holdsworth, and P. Renshaw, "Glass transitions of hygrothermal aged pultruded glass fibre reinforced polymer rebar by dynamic mechanical thermal analysis," *Materials & Design*, vol. 42, pp. 272–278, 2012.

[49] O. Gooranorimi, W. Suaris, E. Dauer, and A. Nanni, "Microstructural investigation of glass fiber reinforced polymer bars," *Composites Part B: Engineering*, vol. 110, pp. 388–395, 2017.

[50] C.-G. Park, C.-I. Jang, S.-W. Lee, and J.-P. Won, "Microstructural investigation of long-term degradation mechanisms in GFRP dowel bars for jointed concrete pavement," *Journal of Applied Polymer Science*, vol. 108, no. 5, pp. 3128–3137, 2008.

[51] D. Miller, J. Mandell, D. Samborsky, B. Hernandez-Sanchez, and D. T. Griffith, "Performance of composite materials subjected to salt water environments," in *Proceedings of the 53rd AIAA/ASME/ASCE/AHS/ASC Structures, Structural Dynamics and Materials Conference*, American Institute of Aeronautics and Astronautics, Honolulu, HI, USA, 2012.

[52] M. Abhijit and S. J. Arwikar, "Performance of glass fiber-reinforced polymer reinforcing bars in tropical environments-Part I: structural scale tests," *ACI Structural Journal*, vol. 102, no. 5, pp. 745–753, 2005.

[53] C. E. Bakis, A. J. Freimanis, and D. Gremel, "Effect of resin material on bond and tensile properties of unconditioned and conditioned FRP reinforcement rods," in *Proceedings of the 1st International Conference on durability of Fiber Reinforced Polymer (FRP) Composites for Construction*, Sherbrooke, QC, Canada, 1998.

[54] C. E. Bakis, T. E. Boothby, R. A. Schaut, and C. G. Pantano, "Tensile strength of GFRP bars under sustained loading in concrete beams," *ACI Special Publication*, vol. 230, pp. 1429–1446, 2005.

[55] M. G. Phillips, "Prediction of long-term stress-rupture life for glass fibre-reinforced polyester composites in air and in aqueous environments," *Composites*, vol. 14, no. 3, pp. 270–275, 1983.

[56] B. Benmokrane, P. Wang, T. M. Ton-That, H. Rahman, and J. Francois, "Durability of glass fiber-reinforced polymer reinforcing bars in concrete environment," *Journal of Composites for Construction*, vol. 6, no. 3, 2002.

[57] JSCE, "Recommendations for design and construction of high performance fiber reinforced cement composites with multiple fine cracks (HPFRCC)," in *Concrete Engineering Series 82*, Japan Society of Civil Engineers, Japan, 2008.

[58] CSA S6, *Canadian Highway Bridge Design Code*, Canadian Institute of Steel Construction, Canada, 2014.

[59] NS 3473, *Concrete structures-Design and Detailing Rules*, Norsk Standard, Norway, 2003.

[60] CSA S806, *Design and Construction of Building Structures with Fibre-Reinforced Polymers*, Canadian Standards Association, Canada, 2017.

[61] J. Huang and R. Aboutaha, "Environmental reduction factors for GFRP bars used as concrete reinforcement: new scientific approach," *Journal of Composites for Construction*, vol. 14, no. 5, pp. 479–486, 2010.

[62] ACI Commitee 440.6, *Specification for Carbon & Glass Fiber-Reinforced Polymer Bar Materials for Conc Reinforcement (Metric)*, American Concrete Institute, Farmington Hills, MI, USA, 2008.

[63] CSA S807, *Specification for Fibre-Reinforced Polymers*, Canadian Standards Association, Canada, 2015.

[64] Y. A. Al-Salloum and T. H. Almusallam, "Creep effect on the behavior of concrete beams reinforced with GFRP bars subjected to different environments," *Construction and Building Materials*, vol. 21, no. 7, pp. 1510–1519, 2007.

[65] H. Fergani, M. Di Benedetti, C. Miàs Oller, C. Lynsdale, and M. Guadagnini, "Long-term performance of GFRP bars in concrete elements under sustained load and environmental actions," *Composite Structures*, vol. 190, pp. 20–31, 2018.

[66] T. D'Antino, M. A. Pisani, and C. Poggi, "Effect of the environment on the performance of GFRP reinforcing bars," *Composites Part B: Engineering*, vol. 141, pp. 123–136, 2018.

[67] J. L. Thomason, "The interface region in glass fibre-reinforced epoxy resin composites: 2. Water absorption, voids and the interface," *Composites*, vol. 26, no. 7, pp. 477–485, 1995.